Iranian Journal of Medical Physics

ijmp.mums.ac.ir

Design and Development of an Anthropomorphic Heterogeneous Female Pelvic (AHFP) Phantom for Dosimetric Verification of Advance Radiotherapy

Neha Yadav[1,3*], Manisha Singh[1], Surendra Prasad Mishra[2], Mohammad Shanawaz Ansari [3], Atul Mishra[4]

1. Department of Applied Physics, Amity School of Engineering & Technology, Amity University Madhya Pradesh, Maharajpura Dang, Gwalior, India
2. Department of Radiation Oncology, Dr. RMLIMS, Lucknow, India
3. Department of Medical Physics, Apollo Hospitals Bilaspur, Chhattisgarh, India
4. Department of Radiation Oncology, Uttar Pradesh University of Medical Sciences, Saifai, Etawah (U.P.) - 206130, INDIA

A R T I C L E I N F O

Article type:
Original Paper

Article history:
Received: Oct 12, 2022
Accepted: Jan 22, 2023

Keywords:
Homogeneous Phantom
Heterogeneous Phantom
Radiation Dosimetry

A B S T R A C T

Introduction: The objective of this work is to design a new kind of AHFP phantom to determine if this phantom is a realistic representation of actual cervical cancer patients. This can serve as a stand-in for the dosimetry quality assurance of a real patient.

Material and Methods: An anthropomorphic heterogeneous female pelvic phantom was designed which was made of paraffin wax, a female pelvic bone, water, gauze, polyvinyl chloride (PVC) and polymerized siloxanes. The AHFP phantom was scanned using a CT scanner (Toshiba Alexion 16 multi–Slice CT scanner) at 120kVp and 250mAs with a slice thickness of 2mm to assess how accurately the resulting phantom product simulates a real patient. The CT images were transferred to the Eclipse treatment planning system for dosimetry analysis.

Results: The AHFP phantom's CT numbers and relative electron densities of the uterus, bladder, rectum, muscles, fat, bones, and cavities were found close to real patients. The mean percentage variations between planned and measured doses of all RapidArc QA plans were of 2.14 % and standard deviation of 0.543 (t=0.135, p= 0.447; $p>0.05$) for homogeneous phantom¸ and 7.57% & standard deviation 2.358 (t=4.674, p=0.00094; p< .05) for AHFP phantom.

Conclusion: It is concluded that the existing algorithms in TPS for dosimetry are working fine for homogeneous phantoms, but it does not work good for heterogeneous (AHFP) phantom. Therefore, patient-specific absolute dosimetry should be performed using a heterogeneous phantom that closely resembles the actual human body in terms of both density and design.

► *Please cite this article as:*
Yadav N, Singh M, Mishra SP, Ansari MS, Mishra A. Design and Development of an Anthropomorphic Heterogeneous Female Pelvic (AHFP) Phantom for Dosimetric Verification of Advance Radiotherapy. Iran J Med Phys 2024; 21: 64-70. 10.22038/IJMP.2023.68397.2194.

Introduction

Radiotherapy is a modality of cancer treatment in which ionization radiation is used in the cancer treatment to control or selectively kill the malignant cells. The main goal of the radiotherapy phantom is to replicate the human body as accurately as possible. This helps to increase the precision of radiotherapy and calculate how much radiation is absorbed by the body. Radiotherapy phantom should be made of materials that absorbs and scatters-radiation in the same way as the real tissues do [1-4]. Water was the first tissue equivalent material which was used in radiation measurements by kienbock [5]. It is a desired medium for dose measurements for several reasons. It is nearly tissue equivalent, easily available and inexpensive. The first formulated Solid Phantom's material called Siemen's Wax, made up of paraffin wax and magnesium oxide as a corrective filter, was reported by Ott in 1937 [6].A Synthetic wood or other rigid materials based phantoms were used for radiation dosimetry which are approximately tissue equivalent but these phantoms do not have skeletons and also materials are not stable with respect to tissue- equivalence. With the advent of rapid development of highly conformal radiation therapy, modern radiation therapy requires high geometrical precision of radiation delivery. At the same time, the complexity of treatment of planning software has substantially increased and the trend towards innovative body phantom design continued with introduction of two elaborate adult-sized body phantoms, the 'Temex' and the 'Rando' [7]. They had real skeletons, body cavities, and artificial lungs, with slices that enabled the evaluation of radiation dose-distributions. Those were used to predict to radiation exposure to humans during radiation therapy [8]. But these phantoms are commercially very expensive. The

**Corresponding Author:* Tel: *+91*-8889781816; Email: nehadav51990@gmail.com

objective of this work is to design the new kind of an anthropomorphic heterogeneous pelvic phantom that closely resembles the anatomy of cervical cancer patient. This phantom can be used as a pre-treatment quality assurance tool for advance radiotherapy.

Materials and Methods

Phantom design

In this study, an anthropomorphic heterogeneous female pelvic phantom was designed (Figure 1) which was made of paraffin wax, a female pelvic bone, water, gauze, polyvinyl chloride (PVC) and polymerized siloxanes. The internal organs such as uterus made of polymerized siloxanes with wax, bladder made of balloon filled with 250 ml water and rectum made of cylindrical PVC hollow pipe filled with gauze and paraffin wax. The phantom was made in five sequential steps: (1) The female pelvic dummy was made up of thermoplastic sheets and tough cloth tape, (2) The internal organs, including the uterus, bladder, and rectum, were positioned within the female pelvic bone and securely fastened with gypsum bandages. The density of the female pelvic bone is equivalent to that of a human pelvic bone.(3) The internal organs and pelvic bones were placed in the female pelvic dummy at right anatomical positions, (4) the liquid paraffin wax was poured in the pelvic dummy for surface mold and the whole assembly was left for cooling and stabilization. The AHFP phantom in its final form is depicted in Figure 1. (5) A cavity was meticulously prepared, positioned approximately in the area corresponding to the uterus in the phantom. To precisely define the dimensions of this cavity, a 0.60cc ion chamber (PTW, Freiburg, Germany) was positioned in the same location. The establishment of three reference points was facilitated by the placement of fiducial lead markers. Specifically, two markers were symmetrically positioned on bilateral points, while the third was placed anteriorly on the phantom's surface. All markers were aligned within the same cross-sectional plane to ensure precise localization. The physical dimensions of the phantom are 22.5 cm anterior–posterior separation at the uterus region, 30.5 cm separation laterally at that point and about 31.5 cm in the vertical dimension, where the extent is from the lower abdomen to the upper thigh region. The phantom is about 15 kg in weight.

Physical and radiological properties

The AHFP phantom was scanned using a CT scanner (Toshiba Alexion 16 multi Slice CT scanner) at 120 kVp and 250 mAs with a slice thickness of 2mm in order to assess how accurately the resulting phantom product simulates a real patient. To the Eclipse treatment planning system, the CT scans were uploaded (version 11.0.31). The CT scans of the phantom were compared to the CT images of cervical cancer patients who were chosen randomly and underwent similar scanning conditions (120kVp, 250mAs, and 2 mm slice thickness). The organs delineation such as rectum, bladder, uterus and bone on AHFP phantom are shown in the Figure 2.

Figure 1. AHFP Phantom setup on Clinac iX Varian Machine

Table 1 presents the average and standard deviation of CT numbers measured in Hounsfield units (HU) for both patient and phantom CT images. The determination of relative electron density for the materials was carried out using the provided formulas denoted as (i) and (ii) [9].

P_e=HU/1000+1 HU< 100 (i)

P_e = HU/1950+1 HU≥ 100 (ii)

Where pe is the relative electron density of the materials.

Radiation dosimetry using AHFP phantom with commercially available homogeneous phantom

For the patient-specific absolute dosimetry of completed RapidArc treatment plans, two distinct phantoms were selected. The first phantom, illustrated in Figure 3(A), was a homogeneous "Water–equivalent RW3 solid phantom" from PTW Freiburg, Germany. Each slab of this phantom was constructed from polystyrene with an effective atomic number of 5.74. The second phantom, depicted in Figure 3(B), was the AHFP phantom. In this case, the density of the internal organs in the AHFP phantom closely matched that of the human pelvic region. The CT scans of both phantoms were conducted on a Toshiba Alexion 16 multi-slice CT scanner, featuring a slice thickness of 2 mm for planning purposes. These CT images were then imported into the Eclipse Treatment Planning System (TPS) version 11.0.31 (Varian Medical Systems, Palo Alto, CA). The previously devised RapidArc plans for patient treatment were exported to both phantoms, as illustrated in Figure 3.

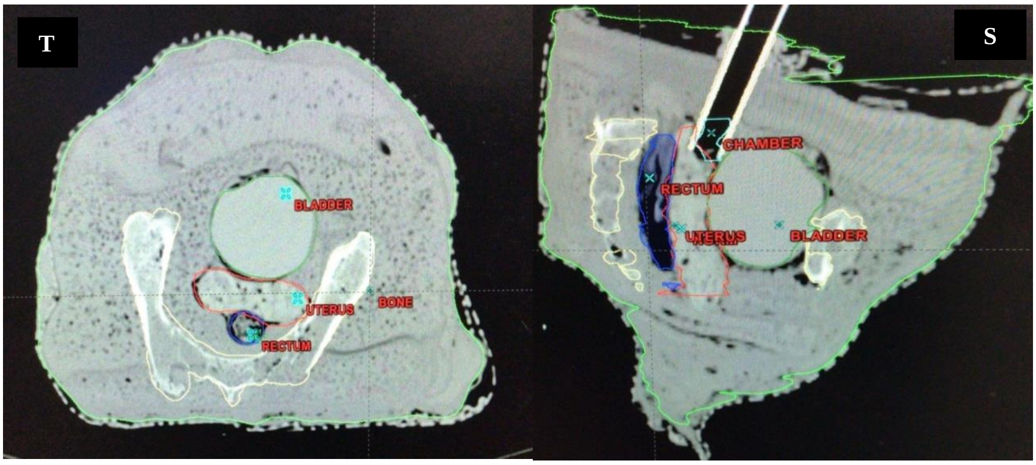

Figure 2. Transversal (T) and Sagittal (S) CT view of Organs Delineation on AHFP Phantom

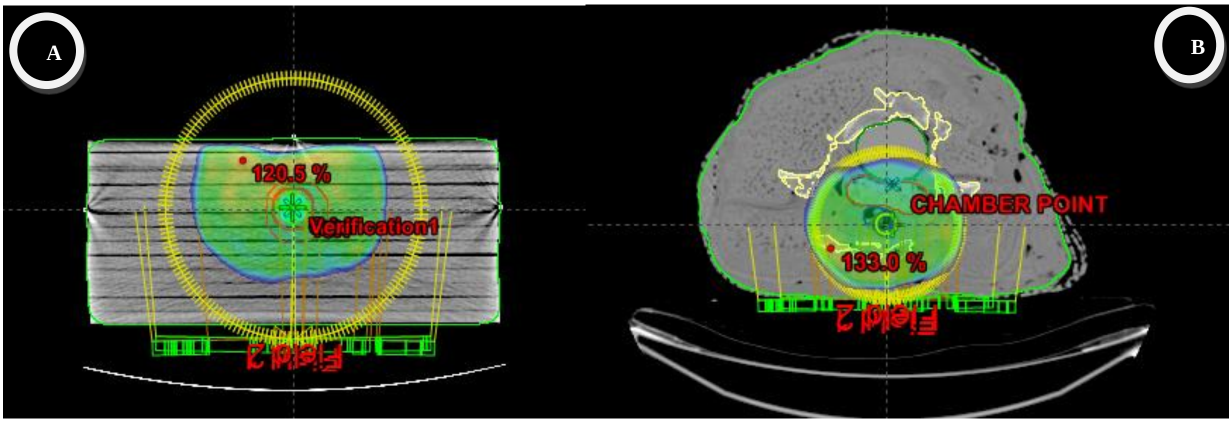

Figure 3. (A)RapidArc plan on homogeneous phantom (Slab Phantom), (B) RapidArc plan on AHFP Phantom

All selected plans were designed with a 6 MV photon beam, and the field arrangement ensured that all fields were coplanar with a couch angle of 0°. The plan optimization utilized the Dose Volume Optimizer (DVO), and dose calculations were performed using the Anisotropic Analytical Algorithm (AAA) version 11.30.1, employing a grid size of 0.25 cm. Subsequently, all plans were delivered, and the dose for each plan was measured using a PTW UNIDOSE electrometer coupled with a 0.6 cc ionization chamber from IBA Dosimetry Germany, securely fixed within the phantoms. This comprehensive process ensured the meticulous verification and validation of the RapidArc treatment plans, using both the Water–equivalent RW3 solid phantom and the AHFP phantom for patient-specific dosimetry.

The percentage (%) deviation between the measured dose on the linear accelerator and the planned dose on the Treatment Planning System (TPS) was determined using the following formula:

$$Percentage\ of\ Variation = \frac{(Mesasured\ Dose\ at\ Linac - TPS\ Planned\ Dose)X100}{TPS\ Planned\ Dose}$$

This calculation enabled the assessment of variations between the actual measured dose during linear accelerator delivery and the originally planned dose in the TPS.

Statistical analysis

The differences between the two groups' various parameters were analyzed statistically using a Microsoft excel 2010 spreadsheet using the two-sample t-test (where $P<0.05$ was regarded statistically significant).

Results

Physical Dimensions

When compared to the average values measured in a sample of roughly thirty patients, the surface and interior organ dimensions of the AHFP phan tom are accurate to within 2 millimetres (Table 1). The manufactured anthropomorphic heterogeneous female p elvic phantom's internal organ positions relative to the U mbilicus landmark are comparable, as shown in Table 2. The distances between structures and bone landmarks a re also found to be equivalent to values seen in CT scans of patients with cervical cancer.

Radiological Properties of the AHFP Phantom

The comparison between measured CT numbers (HU) and relative electron density (RED) for various anatomical structures, including the uterus, bladder, rectum, muscles, fat, bones, and cavities, across both the AHFP phantom and patient groups reveals a strong agreement. The results of this comparative analysis are presented in Table 3, showcasing the alignment between the measured CT numbers of a randomly selected sample of patients from our institution and the phantom. This indicates that the AHFP, designed for this study, aligns well with both the qualitative and quantitative aspects of CT evaluation.

Radiation dosimetry using AHFP phantom with commercially available homogeneous phantom

The mean percentage variations between planned and measured doses of all rapid arc QA plans were as 2.14% and standard deviation 0.543 for slab phantom (t=0.135, p=0.447 ; $p>0.05$) and 7.57% & SD 2.358 (t=4.674, p=0.00094; p<0.05) for AHFP phantom. Results in details are given in the Table 4. The comparative study of percentage of variation between homogeneous slab phantom and AHFP phantom represents in Figure 4.

Table 1. Physical dimensions of the phantom and real patients

Organs	Dimension of real female pelvic	Dimension of AHFP Phantom
	Dim.(Mean±SD) in cm	
Surface		
Length (Lower Abdomen to upper thigh)	31.02±0.79	31.50
Width	30.62±2.2	30.5
Separation	20.1±2.1	22.5
Bladder (Oval Shape)		
Length	6.5±1.5	7.5
Width	5±0.5	7.0
Thickness	4±0.5	6
Rectum (Cylindrical shape)		
Length	12.5±1.5	12.0
Width	4.5±0.7	
Thickness	3.5±0.8	
Uterus		
Length	8±0.7	
Width(U)		11.0
(M)	4.5±1.6	
(L)	5.5±0.7	7.0
	3±0.4	6.0
Thickness		3.5
(U)	3±0.7	
(M)	3.8±0.7	
(L)	2.5±0.5	2.5

Table 2. Internal organs' distance from the pubic symphysis

S.N.	Organ	Distance in cm in real female pelvis(Mean±SD)	AHFP Phantom
1	Bladder	4.2±0.7	3.8
2	Uterus	8.4±1.5	7.8
3	Rectum	12.5±1.4	11.5

Table 3. Measurement of the CT Number (HU) and Relative Electron Density (RED) of Developed AHFP Phantom and Real Patient

S.N.	Pelvic Organs	Actual Female Patient		AHFP Phantom	
		HU±SD	RED	HU±SD	RED
1	Muscles	62±15	1.05	74±28	1.11
2	Fats	-106±15	0.945	-168±81	0.908
3	Uterus	38±18	1.04	48±18	1.05
4	Rectum	37±17	1.04	41±27	1.07
5	Bladder	11±5	1.01	-5±15	1.01
6	Bone	951±121	1.49	946±281	1.63

Table 4. The Comparision of Patient-Specific Absolute Dosimetry using Homogeneous (Slab Phantom) Phantom and AHFP Phantom

S.N.	Homogeneous Phantom (Slab Phantom)			Heterogeneous Phantom (AHFP Phantom)		
	Planned Dose on TPS (cGy)	Measured Dose on LA (cGy)	% of Variation	Planned Dose on TPS (cGy)	Measured Dose on LA (cGy)	% of Variation
1	198.02	195.32	-1.363	202	185	-8.42
2	199.50	193.99	-2.761	210	190.5	-9.29
3	193.42	190.50	-1.51	212	192.36	-9.26
4	228.60	231.90	+1.44	202	194.5	-3.71
5	199.82	203.84	+2.012	195	187.35	-3.92
6	214.52	212.32	-1.025	213.62	196.34	-8.09
7	186.01	181.63	-2.355	204.39	193.89	-5.14
8	218.13	224	2.691	191.6	171.89	-10.29
9	204.2	198.62	-2.733	212	194.56	-8.23
10	206.07	211	+2.392	209.96	191.65	-8.72
Average Value		2.14%		7.57%		
Standard Deviation		0.543		2.358		
t-value		0.135		4.674		
p-value		0.447		0.00094		

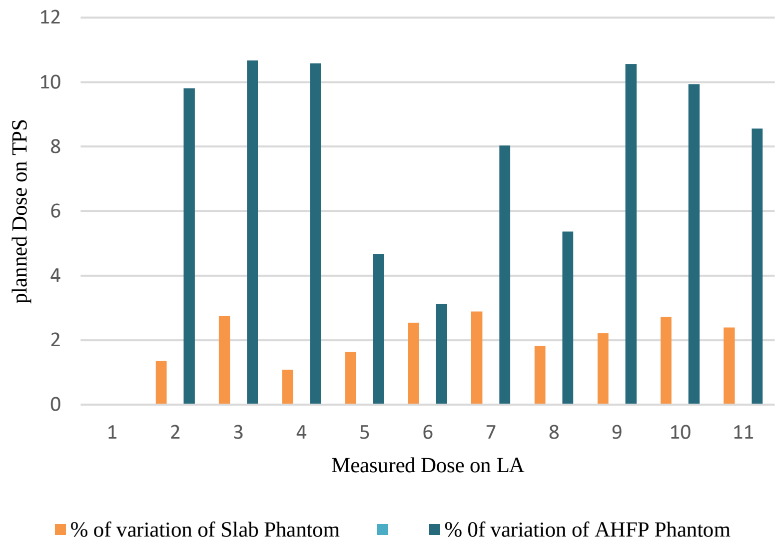

Figure 4. Percentage Variation in Dosimetry between Homogeneous Slab Phantom and AHFP Phantom

Discussion

This study aimed to develop a three-dimensional anthropomorphic heterogeneous female pelvic phantom for dosimetry verification. In this study, the Hounsfield Unit (HU) or CT Number and relative electron density (RED) of a created phantom were compared to those of a real patient's CT scan. This study also looked into how tissue heterogeneities affected dosage calculations. The study's findings showed that the created phantom was identical to an actual patient, and the materials used to build it were readily available and reasonably priced.

According to Inderjeet Singh et al. [10], the measurements of the female hip width was 18.6 cm, the bladder was 5 cm, the uterus was 7.5 cm long, 5 cm width, and 2.5 cm thick,[11-12] and the rectum was 15 cm[13], all of which are in good agreement with the measurements found in this study. The sagittal distance of the bladder, uterus, and rectum in both the real female pelvis and the locally designed AHFP phantom were also measured on CT-axial slices during the course of this study. These measurements revealed that the distances were, respectively, 3.8 cm, 7.8 cm, and 11.5 cm. The Hounsfield number for human muscles has been calculated by J. F. Winslow et al. [14] as well as the soft tissue equivalent substitution range of -50 to -150 and the bone tissue equivalent substitution range of 650.These findings align with the findings of our investigation Adipose, muscle, and bone relative electron densities were also calculated by C. D. Trujillo et al [15] and N. Kanematsu [16] and found to be (0.96, 1.04, 1.31) and (0.952, 1.04, 1.116) respectively. These values are also in good agreement with our observed values of (0.913, 1.105, and 1.628), which are respectively. D Shrotriya et al. [17] also calculated the relative electron densities of the bladder, rectum, fat, and bone, which were reported to be 1.305, 1.025, 0.913 and 1.579 respectively. These conclusions are similarly consistent with the study's observed values of 1.07, 1.015, 0.909 and 1.628 respectively, with a minor variance. These findings were also estimated by S. Singh et al. [18] and find no variation in bladder, rectum, fat and bone which were reported 1.037, 1.051, 0.896 and 1.632 respectively. During the course of the research, we observed that the Hounsfield Unit (HU) and relative electron density values of our locally developed female pelvic phantom closely resemble those of a human female pelvis [19-21]. For the homogeneous slab phantom, the percentage difference between planned and measured doses was below 3%, with a standard deviation of 0.543 (t=0.135, p= 0.447), indicating non-significance at $p< 0.05$. Conversely, deviations in planned and measured doses for the AHFP phantom were 10.29% (maximum value), 3.71% (minimum value), and 7.57% (average value), with a standard deviation of 2.358 (t=4.674, p=0.00094), highlighting significance at $p<0.05$. The percentage of variation between the homogeneous slab phantom and AHFP phantom revealed a t-value of -7.012, with a p-value < .00001, signifying significance at $p<0.05$. Notably, these outcomes underscore the impact of heterogeneous media, as depicted in Figure 4.

Many physicists currently adhere to established standards outlined in guidelines such as AAPM Task Group Report 120, TRS 398, and ICRU 83 [22]. These guidelines recommend water-equivalent phantoms, given that the adult human body consists of approximately 70% water, varying with factors like age, sex, and body composition. However, a phantom with full water-equivalent density may not accurately represent the diverse tissues and cavities found in the human body, including pelvic structures such as pelvic bone, femoral heads, rectum, bladder, and bowels, each possessing distinct radiological properties. The recognizing these variations is crucial for precisely predicting the delivered dose to all irradiated tissues, especially when aiming to maximize therapeutic benefits in the presence of such heterogeneities during radiation therapy.

These heterogeneities disarrange the dose-distribution in the target during radiation therapy. But at the time of verification of patient specific quality assurance, the algorithms in TPS assume the human body homogeneous in nature. Therefore, an intensive dosimetry is mandatory during the execution of the treatment techniques and pre-treatment patient verification processes. This type of treatment accuracy and precision of dose delivery can be achieved when an anthropomorphic designed phantom is available. However, none of the commercially available homogeneous phantoms simultaneously satisfy all of the dosimetry requirements. To validate the accuracy of dose calculations performed by Treatment Planning System (TPS) algorithms for individual patients, it is essential to conduct patient-specific absolute dosimetry using phantoms that mimic the heterogeneous density of the human body. This approach ensures a more realistic representation and assessment of the computed radiation dose in diverse patient scenarios.

Conclusion

In conclusion, our research introduced and designed an anthropomorphic heterogeneous female pelvic (AHFP) phantom, revealing its close resemblance to the physical and radiobiological properties of a real patient's pelvic region. A notable increase in dose variation was observed in the AHFP phantom compared to a homogeneous slab phantom. The study concludes that while existing dosimetry algorithms perform well for homogeneous phantoms, they exhibit limitations for heterogeneous (AHFP) phantoms. Therefore, patient-specific absolute dosimetry is recommended using a phantom that accurately simulates both the density and anatomical design of the human body.

References

1. FM Khan, The Physics of Radiation Therapy, fourth ed., Philadelphia, Wolters Kluwer. 2012.
2. The ICRU Report 83, prescribing, recording, and reporting photon beam intensity-modulated radiation therapy (IMRT), Cancer/Radiotherapy. 2011; 15(6-7): 555–9.
3. Fraass B, Doppke K, Hunt M, Kutcher G, Starkschall G, Stern R, et al. American Association of Physicists in Medicine Radiation Therapy Committee Task Group 53: quality assurance for clinical radiotherapy treatment planning. Medical physics. 1998 Oct;25(10):1773-829.
4. Kutcher GJ, Coia L, Gillin M, Hanson WF, Leibel S, Morton RJ, et al. Comprehensive QA for radiation oncology: report of AAPM radiation therapy committee task group 40. MEDICAL PHYSICS-LANCASTER PA-. 1994 Apr 1;21:581-618.
5. Kienbock R. On the quantimetric method. Archives of the Roentgen Ray. 1906 Jun 1;11(1):17-20.
6. Ott P. Zur Röntgenstrahlenbehandlung oberflächlich gelagerter Tumoren; Ott, Paul, Dr. phil. Dr. med. L. Schumacher; 1937.
7. Absorbed dose determination in external beam radiotherapy: An international code of practice for dosimetry based on absorbed dose to water. IAEA, Vienna¸ 2000.
8. International Commission on Radiation Units and measurements (ICRU). Tissue substitutes in radiation dosimetry and measurement. Report No. 44. Bethesda, MD, USA. 1998.
9. Thomas SJ. Relative electron density calibration of CT scanners for radiotherapy treatment planning. The British journal of radiology. 1999 Aug;72(860):781-6.
10. Singh I, Rawat S, Varte LR, Majumdar D. Workstation Related Anthropometric and Body Composition Parameters of Indian Women of Different Geographical Regions. Journal of Krishna Institute of Medical Sciences (JKIMSU). 2015 Jan 1;4(1).
11. Gray H. Anatomy of the Human Body (Bladder). Lea & Febiger; 1878.
12. Gray H. Anatomy of the Human Body (Uterus). Lea & Febiger; 1878.
13. Theakston V. The Rectum. Available from:http://techmeanatom.info/abdomen/gi-tract/rectum.

14. Winslow JF, Hyer DE, Fisher RF, Tien CJ, Hintenlang DE. Construction of anthropomorphic phantoms for use in dosimetry studies. Journal of Applied Clinical Medical Physics. 2009 Jun;10(3):195-204.
15. Trujillo-Bastidas CD, García-Garduño OA, Lárraga-Gutiérrez JM, Martínez-Dávalos A, Rodríguez-Villafuerte M. Effective atomic number and electron density calibration with a dual-energy CT technique. InAIP Conference Proceedings. 2016; 1747(1).
16. Kanematsu N. Relationship between mass density, electron density, and elemental composition of body tissues for Monte Carlo simulation in radiation treatment planning. Physics in Medicine and Biology. 2016; 61(13):5037-50.
17. Shrotriya D, Yadav RS, Srivastava RNL, Verma TR. Design and Development of an Indigenous In-house Tissue-equivalent Female Pelvic Phantom for Radiological Dosimetric Applications. Iran J MedPhys. 2018; 15:200-5.
18. Singh S, Raina P, Gurjar OP. Dosimetric Study of an Indigenous and Heterogeneous Pelvic Phantom for Radiotherapy Quality Assurance. Iran J Med Phys. 2020; 17: 120-5.
19. Branco, Daniela. Development and Implementation of an Anthropomorphic Head & Neck Phantom for the Assessment of Proton Therapy Treatment Procedures. UT GSBS Dissertations and Theses (Open Access). 2016; 689.
20. Zhang F, Zhang H, Zhao H, He Z, Shi L, He Y, et al. Design and fabrication of a personalized anthropomorphic phantom using 3D printing and tissue equivalent materials. Quantitative imaging in medicine and surgery. 2019 Jan;9(1):94.
21. Singh I, Rawat S, Varte LR, Majumdar D. Workstation Related Anthropometric and Body Composition Parameters of Indian Women of Different Geographical Regions. Journal of Krishna Institute of Medical Sciences (JKIMSU). 2015 Jan 1;4(1).
22. ICRU Report 83. Prescribing¸ recording¸ and reporting photon-beam intensity-modulated radiation therapy (IMRT). International Commission on Radiation Units and Measurements¸ Bethesda; 2010.